ELSEVIER

www.elsevier.nl/locate/jorganchem

Journal of Organometallic Chemistry 593–594 (2000) 431–444

Journal of Organometallic Chemistry

Pd(II) and Rh(I) chelate complexes of the bidentate phosphino–thiourea ligand $PhNHC(S)NHCH_2CH_2PPh_2$: structural properties and activity in homogeneous and hybrid catalysis

Daniele Cauzzi [a], Mirco Costa [b], Nicola Cucci [a], Claudia Graiff [a], Federica Grandi [a], Giovanni Predieri [a], Antonio Tiripicchio [a,*], Roberto Zanoni [c]

[a] *Dipartimento di Chimica Generale ed Inorganica, Chimica Analitica, Chimica Fisica, Università di Parma, Centro di Studio per la Strutturistica Diffrattometrica del CNR, Parco Area delle Scienze 17A, I-43100 Parma, Italy*
[b] *Dipartimento di Chimica Organica e Industriale, Università di Parma, Parco Area delle Scienze 17A, I-43100 Parma, Italy*
[c] *Dipartimento di Chimica, Università di Roma 'La Sapienza', Piazzale Aldo Moro 5, I-00185 Rome, Italy*

Received 2 August 1999; accepted 13 October 1999

Dedicated to Professor Fausto Calderazzo on the occasion of his 70th birthday, in recognition of his outstanding contributions to inorganic and organometallic chemistry.

Abstract

The new bifunctional ligand $PhNHC(S)NHCH_2CH_2PPh_2$ (Ptu), containing the thiourea and the phosphine functions, and its Pd(II) and Rh(I) complexes were prepared. Ptu behaves as a bidentate ligand forming seven-membered chelation rings in a boat-like conformation. In the case of palladium, this was ascertained by the X-ray determination of the structure of the complexes $[Pd(Ptu)_2]Cl_2 \cdot 6CHCl_3$ (**1**), $[Pd(Ptu)_2Cl]Cl \cdot EtOH$ (**2**) and $[Pd(Ptu)_2][CoCl_4] \cdot CHCl_3 \cdot 2EtOH$ (**3**). In complexes **1** and **3**, the two ligands are related centrosymmetrically, whereas in **2** they are folded by the same side in an *umbrella* arrangement. The Rh(I) complexes [Rh(cod)(Ptu)]X (X = Cl or PF_6; cod = 1,5-ciclooctadiene) and $[Rh(cod)(Ptu)]_2[CoCl_4]$ were characterized by ^{31}P-NMR and FT-IR spectroscopy. The catalytic activity in homogeneous hydrogenation and hydroformylation reactions of the Pd(II) and Rh(I) complexes was dependent on the counter-anion, being very low in the case of Cl^- and high in the case of non-coordinating anionic groups such as $CoCl_4^-$ and PF_6^-. The related ligand $(EtO)_3Si(CH_2)_3NHC(S)NHCH_2CH_2PPh_2$ (SiPtu) was sol-gel processed giving hybrid inorganic–organic xerogels (XGPtu). Anchored Pd(II) and Rh(I) complexes were obtained by two procedures: by treating XGPtu with solution of precursor complexes or by sol-gel processing previously prepared SiPtu complexes. Palladium complexes of the thiourea ligand $(EtO)_3Si(CH_2)_3NHC(S)NHPh$ (Siphtu), with different S–Pd ratios, were also sol-gel processed. The rhodium containing xerogel was found to be an active catalyst for the hydroformylation of styrene, but metal leaching occurred, even if to a limited extent. In the case of Pd-containing materials, it was ascertained that the heterogeneous hydrogenating activity depends on the presence of colloidal metal particles, which form when the metal species are not adequately surrounded by the P,S- or S-ligands.

Keywords: Thiourea functions; Bidentate ligand; Umbrella arrangement; Sol-gel materials

1. Introduction

The design and the production of new heterogeneous catalysts are of major interest in chemistry and chemical engineering. They should allow the development of new chemical processes which are of economical, as well ecological interest, to the chemical industry [1]. In particular, the immobilization of transition metal complexes to polymeric matrices leads to systems that are able to combine the advantages of homogeneous and heterogeneous catalysis (hybrid catalysis) [2]. In this regard, the sol-gel process has been proved to offer the possibility for the preparation of suitable polymeric frameworks under smooth and low temperature conditions [3].

* Corresponding author. Fax: +39-0521-905557.
E-mail address: tiri@unipr.it (A. Tiripicchio)

0022-328X/00/$ - see front matter
PII: S0022-328X(99)00615-4

In previous works we have synthesized the novel thiourea-functionalized silica xerogels represented in the Scheme 1, in order to have polymeric materials designed to support soft-metal species through coordinative linkage.

These xerogels are able to bind palladium(II) [4], copper(I) and (II) [5], rhodium(I) [6] and metal carbonyl species [4], including clusters [7]. The rhodium containing materials are effective, recyclable hydroformylation hybrid catalysts, styrene being quantitatively converted into the corresponding linear and branched aldehydes; there is spectroscopic evidence that anchored rhodium(I) complexes are the active species [6b]. In further experiments [8], we have observed that certain catalysts of this family show significant changes in regioselectivity after consecutive catalytic runs. XPS and EDX data strongly suggest that surface metal leaching occurs to a certain extent, in such a way that the hydroformylation reaction is forced to move progressively from the xerogel surface to the inside of the matrix, where different environments could be responsible for the observed selectivity.

On the other hand, the system Pd/XGphtu behaves as an excellent recyclable hydrogenation catalyst, showing a remarkable selectivity in converting alkynes to the corresponding alkenes [4]. TEM investigations carried out on this system after some catalytic runs have revealed the presence of colloidal palladium particles, ranging in size from about 10–20 nm, dispersed uniformly throughout the siloxane matrix. In the case of the benzoylthiourea function, the nature of the palladium aggregates has been investigated by means of CO absorption, DRIFTS, XPS and TEM techniques [9].

As an extension of these investigations, we have synthesized the new bifunctional ligand PhNHC(S)NHCH$_2$CH$_2$PPh$_2$ (Ptu) containing both the thiourea and the phosphine functions. Ptu is a potential P,S-bidentate ligand which can form seven-membered chelation rings.

Similar molecules, such as PhNHC(S)NH(CH$_2$)$_3$PPh$_2$ and PhNHC(S)NH(CH$_2$)$_3$PHPh [10] are reported in the literature, but, as far as we know, no metal complexes have been structurally characterized and tested as catalysts. Regarding bifunctional thioureas, systematic studies have been carried out on *N*-acylthioureas, showing the coordination versatility of these molecules [11]. Other molecules containing the CS and P donating groups have been studied as ligands, for instance those of the family X$_2$NC(S)NX$_2$ (X = H, PR$_2$) [12]. Furthermore, certain complexes of P,S-bidentate ligands, such as Ph$_2$PCH$_2$P(S)Ph$_2$, have displayed remarkable activity in the catalytic carbonylation of methanol [13].

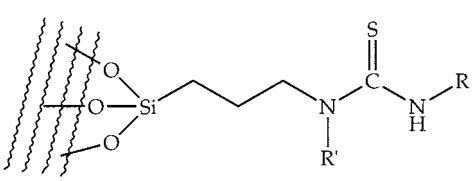

XGphtu	R = Ph, R' = H
XGditu	R = Ph, R' = (CH$_2$)$_2$NHC(S)NHPh
XGbztu	R = C(O)Ph, R' = H
XGphenditu	R = (C$_6$H$_4$)NHC(S)NH(CH$_2$)$_3$SiO$_{3/2}$, R' = H

Scheme 1.

This paper deals with the synthesis and characterization of the Pd(II) and Rh(I) complexes of Ptu and of the hybrid materials (XGPtu) obtained by sol-gel processing the related ligand (EtO)$_3$Si(CH$_2$)$_3$NHC(S)NHCH$_2$CH$_2$PPh$_2$ (SiPtu) and its complexes. The catalytic activity of the molecular complexes and of the hybrid xerogels has been tested in the hydrogenation of phenylacetylene (Pd) and the hydroformylation of styrene (Rh). Moreover, the hydrogenating activity of the Pd containing xerogel catalysts has been compared with that of the corresponding materials functionalized with the simple thiourea function –NHC(S)NHPh (XGphtu).

2. Experimental

2.1. Materials and analytical equipment

PhNHC(S)NHPh (Phtu) and (EtO)$_3$Si(CH$_2$)$_3$NHC(S)NHPh (Siphtu), were prepared as reported in the literature [6b,8]. All the other organic and organometallic reagents were pure commercial products. The solvents were reagent grade and were dried and distilled by standard techniques before use. When needed, manipulations of sensitive reagents were carried out under dry nitrogen by means of standard Schlenk-tube techniques.

CHNS elemental analyses were performed with a Carlo Erba EA 1108 automated analyzer. IR spectra were recorded on a Nicolet 5PC FT spectrometer. ^{1}H- and ^{31}P-NMR spectra were obtained with Bruker AC-100, AC-300 and CPX-200 instruments.

The hydroformylation reactions were performed in a 50 ml stainless-steel autoclave (Parr) equipped with a magnetic stirrer and thermostated ($\pm$1°C) in a silicone oil bath (Heidolph). Analytical GLC was carried out with a DANI 3900 chromatograph fitted with a methylsilicone coated capillary column (OV101).

XPS spectra were run on a Vacuum Generators ESCALAB spectrometer, equipped with a hemispherical analyzer operated in the fixed analyzer transmission (FAT) mode, with a pass energy of 20 or 50 eV. Al–K$_{\alpha1,2}$ or Mg–K$_{\alpha1,2}$ photons ($h\nu$ = 1486.6 and 1253.6 eV, respectively) were used to excite photo-emission. The binding energy (BE) scale was calibrated by taking the Au 4$f_{7/2}$ peak at 84.0 eV. Correction of the energy shift due to static charging of the samples was accom-

plished by referencing to the C1s line from the residual pump line oil contamination, taken at 285.0 eV. The accuracy of reported BEs was ± 0.2 eV, and the reproducibility of the results was within these values. XPS atomic ratios are relative values, intrinsically affected by a 10% error. The spectra were collected by a DAC PDP 11/83 data system and processed by means of commercial software.

Energy dispersive X-ray (EDX) microanalyses were obtained with a JEOL 6400 EDS Tracor system for electron microscope microanalysis.

2.2. Preparations and reactions

2.2.1. Preparation of $Ph_2PCH_2CH_2NHC(S)NHPh$ (Ptu)

In a 100 ml Schlenk tube, 1 g (4.36 mmol) of $Ph_2PCH_2CH_2NH_2$ dissolved in 25 ml of dry ethanol were added to 590 mg (4.36 mmol) of PhNCS. The final solution was refluxed for 1 h. The solvent was removed under vacuum to leave a white sticky solid which was washed repeatedly with hexane to obtain a white powder. Yield 98%. Melting point: 80–82°C. IR (cm^{-1}, KBr pellet): 3380 s, 3180 s, br (νNH); 3010–3000 m (νCH arom.); 2950 m, 2930 m (νCH alif.) 1536 vs (ν_{as}NCN); 1495 s; 1432 m; 696 s. ^{1}H-NMR (δ, 300 MHz, $CDCl_3$): 7.87 s (1H, N*H*Ph); 7.44–7.12 (15H, arom.); 6.27 t (1H, N*H*CH_2, $J = 5$ Hz); 3.75 m (2H, C*H*$_2$NH), 2.40 t (2H, C*H*$_2$PPh$_2$, $J = 7$ Hz). ^{31}P-NMR (δ, 81 MHz, $CDCl_3$–$CHCl_3$): -21.1 s. Elemental analysis: (%, Anal. Calc. for $C_{21}H_{21}N_2PS$) C, 70.18 (69.21); H, 5.43 (5.81); N, 7.50 (7.69); S, 8.68 (8.80).

2.2.2. Preparation of $(EtO)_3Si(CH_2)_3NCS$

The synthesis was performed following the published method with minor changes [14]. Hexane instead of diethyl ether was used to extract the liquid isothiocyanate which was obtained subsequently as a yellow oil by filtering the suspension and evaporating the solvent in vacuo.

2.2.3. Preparation of $Ph_2PCH_2CH_2NHC(S)NH(CH_2)_3Si(OEt)_3$ (SiPtu)

In a 100 ml Schlenk tube, 1.5 g (6.54 mmol) of $Ph_2PCH_2CH_2NH_2$ were mixed with 15 ml of dry ethanol. To this solution, 1.724 g (6.54 mmol) of $(EtO)_3Si(CH_2)_3NCS$ in 10 ml of dry ethanol were added dropwise and the solution was refluxed for 1 h. The solvent was removed under reduced pressure to give a colorless, very viscous liquid. The product was not purified. IR (cm^{-1}, neat): 3270 m, br (νNH); 3055 mw (νCH arom.); 2974 m, 2926 m, 2888 m (νCH alif.) 1551 s (ν_{as}NCN); 1079 s (νSiO). ^{1}H-NMR (δ, 100 MHz, $CDCl_3$): 7.43–7.10 (10H, arom.); 5.90 s, br (2H, NH); 3.80 q (6H, CH_3CH_2O); 3.58 m (partially covered by the CH_3CH_2O peaks) (2H, PCH_2CH_2NH); 3.16 m (2H, C*H*$_2$NH); 2.40 t (2H, C*H*$_2$PPh$_2$); 1.58 m (2H, $CH_2CH_2CH_2$); 1.19 t (9H, CH_3CH_2O); 0.59 t (2H, SiC*H*$_2$). ^{31}P-NMR (δ, 81 MHz, $CDCl_3$–$CHCl_3$): -22.3 s.

2.2.4. Preparation of $[(Ph_2PCH_2CH_2NHC(S)NHPh)_2Pd]Cl_2$ (PdPtu) and crystals of **1** and **2**

A total of 50 mg (0.28 mmol) of $PdCl_2$ were added to a solution of 205 mg (0.56 mmol) of Ptu in 25 ml of dried ethanol. The stirred suspension was refluxed, until complete dissolution of $PdCl_2$ (4–6 h), filtered on Celite and then evaporated in vacuo giving an orange solid (PdPtu). A saturated ethanol solution of this solid gave crystals of $[(Ph_2PCH_2CH_2NHC(S)NHPh)_2PdCl]Cl\cdot EtOH$ (**2**) after 2 days at -30°C. The same reaction could be carried out with $(PhCN)_2PdCl_2$ in chlorinated solvents: by using $CHCl_3$ or dissolving **2** in $CHCl_3$ and leaving at low temperature, crystals of $[(Ph_2PCH_2CH_2NHC(S)NHPh)_2Pd]Cl_2\cdot 6CHCl_3$ (**1**) were obtained. IR (cm^{-1}, KBr pellet): 3440 m, br; 3193 s, br (νNH); 3052 s (νCH arom.); 2920 (νCH alif.) 1575 vs (ν_{as} NCN). ^{1}H-NMR (δ, 100 MHz, $CDCl_3$): 10.5 s, br (2H, NH); 7.50–7.02 and 6.42 d (15H, arom.); 4.14 s, br (2H, C*H*$_2$NH), 2.80 s, br (2H, C*H*$_2$PPh$_2$). ^{31}P-NMR (δ, 81 MHz, Ethanol-d_5): 33.5 s; ($CDCl_3$): 28.3 s. Elemental analysis: (%, Anal. Calc. for $C_{42}H_{42}Cl_2N_4P_2PdS_2\cdot C_2H_5OH$) C, 56.70 (55.50); H, 5.25 (5.08); N, 5.72 (5.88); S, 7.01 (6.73).

2.2.5. Preparation of $[(Ph_2PCH_2CH_2NHC(S)NHPh)_2Pd][CoCl_4]$ (PdPtuCo) and crystals of **3**

A total of 200 mg (0.22 mmol) of $[(Ptu)_2PdCl_2]$ were dissolved in 10 ml of ethanol giving an orange–red solution. A blue solution, obtained by dissolving 53 mg (0.22 mmol) of $CoCl_2\cdot 6H_2O$ in 10 ml of ethanol, was added to the first one giving a green solution, which was reduced in volume in vacuo giving a green crystalline solid (PdPtuCo). Crystals of **3** were obtained by stratification with $CHCl_3$ of an ethanol solution of PdPtuCo. IR (cm^{-1}, KBr pellet): 3223 m, br; (νNH); 3052 m (νCH arom.); 2918 m (νCH alif.) 1575 vs (ν_{as} NCN). ^{31}P-NMR (δ, 81 MHz, $CDCl_3$): 36 s ($\Delta\nu_{1/2} =$ 170 Hz). Elemental analysis: (%, Anal. Calc. for $C_{42}H_{42}Cl_4CoN_4P_2PdS_2$) C, 47.41 (48.64); H, 4.18 (4.08); N, 5.06 (5.40); S, 6.49 (6.18).

2.2.6. Preparation of $[(Ph_2PCH_2CH_2NHC(S)NHPh)Rh(cod)]Cl$ (RhPtu)

In a Schlenk tube, 67 mg (0.136 mmol) of $[\{Rh(cod)Cl\}_2]$ and 100 mg (0.272 mmol) of Ptu were dissolved in 30 ml of CH_2Cl_2. The orange–yellow solution was stirred for 1 h and then reduced in vacuo to give an orange solid (RhPtu). IR (cm^{-1}, KBr pellet): 3400 w, br 3200 m, br (νNH); 3051 m (νCH arom.);

2920 (νCH alif.) 2875 m, 2828 m (νCH cod) 1572 vs (ν_{as} NCN). ^{1}H-NMR (δ, 300 MHz, $CDCl_3$): 10.20 s, br (1H, NH); 9.96 s, br (1H, NH); 7.37–6.90 (15H, arom.); 5.15 s, br (2H, CH cod); 4.14 m, br (2H, CH_2NH), 3.29 (2H, CH cod) 2.65 s, br (2H, CH_2PPh$_2$); 2.28 (4H, CH_2 cod); 2.00 (4H, CH_2 cod). ^{31}P-NMR (δ, 81 MHz, $CDCl_3$–EtOH): 33.1 d ($^1J_{P,\,Rh} = 150$ Hz). Elemental analysis: (%, Anal. Calc. for $C_{29}H_{33}ClN_2PRhS{\cdot}CH_2Cl_2$) C, 54.35 (51.78); H, 5.37 (5.07); N, 4.20 (4.03); S, 4.61 (4.60). XPS interatomic ratios: Rh/N/P/S/Cl: 1/2.1/1.0/1.2/1.2. XPS Binding Energies (eV): P2p 132.1; S2p 162.8; N1s 400.5; Rh3d5/2 308.9; Cl2p 198.9.

2.2.7. Preparation of [(Ph$_2$PCH$_2$CH$_2$NHC(S)NHPh)Rh(cod)]$_2$[CoCl$_4$] (RhPtuCo)

A total of 150 mg (0.25 mmol) of [(Ptu)Rh(cod)]Cl were dissolved in 20 ml of ethanol giving a yellow solution. A blue solution, obtained by dissolving 29 mg (0.13 mmol) of $CoCl_2 6H_2O$ in 10 ml of ethanol, was added to the first one giving a deep green solution which was reduced in vacuo to give a green powder. IR (cm^{-1}, KBr pellet): 3256 w, br (νNH); 3051 m (νCH arom.); 2918 (νCH alif.) 2917 m, 2830 m, 2877 m (νCH cod) 1568 vs (ν_{as} NCN). ^{31}P-NMR (δ, 81 MHz, CD_2Cl_2–CH_2Cl_2): 33.3 d ($^1J_{Rh,\,P} = 146$ Hz). Elemental analysis: (%, Anal. Calc. for $C_{58}H_{66}Cl_4CoN_4P_2Rh_2S_2$) C, 49.45 (51.5); H, 4.77 (4.92); N, 4.03 (4.14); S, 4.77 (4.74).

2.2.8. Preparation of [(Ph$_2$PCH$_2$CH$_2$NHC(S)NHPh)Rh(cod)]PF$_6$ (RhPtuPF6)

A total of 20 mg (0.033 mmol) of PtuRh and 20 mg (0.11 mmol) of KPF_6 were dissolved in 20 ml of ethanol and stirred for 1 h. Ethanol was removed under reduced pressure and the orange solid was added of CH_2Cl_2, forming an orange solution and white powder (containing potassium chloride), which was filtered off. IR (cm^{-1}, KBr pellet): 3352 m (νNH); 3058 w (νCH arom.); 2921 m (νCH alif.) 2894 m, 2800 m, (νCH cod) 1570 vs (ν_{as} NCN); 841 vs (PF_6^-). ^{31}P-NMR (δ, 81 MHz, $CDCl_3$): 32.8 d ($^1J_{P,\,Rh} = 151$ Hz); -80 septet ($^1J_{P,\,F} = 730$ Hz).

2.2.9. Preparation of **5** SiO$_2$·SiO$_{3/2}$(CH$_2$)$_3$NHC(S)NH(CH$_2$)$_2$PPh$_2$ (XGPtu)

Conditions for gel formation were: H_2O–EtO = 1, [Si] $\approx$ 1 mol l^{-1}, Si(OEt)$_4$ (TEOS)–ligand = 5, Si–F = 100. A total of 1500 mg (3.04 mmol) of SiPtu were added to 3171 mg (15.22 mmol) of TEOS and 20 ml of ethanol. The solution was stirred and then added of 6.8 mg (0.18 mmol) of NH_4F dissolved in 1.26 ml (70.02 mmol) of water. A gel formed after 10–15 min and was left to dry for 1 week. The white xerogel was then ground and washed with water, ethanol and diethyl ether and dried in vacuum. A total of 2.069 g were obtained (99.7% yield considering complete hydrolysis and condensation). IR (cm^{-1}, KBr pellet): 3322 m, br (νOH, νNH); 3071 w, 3057 w, (νCH arom); 2978 w, 2934 w, 2900 w (νCH aliph.); 1553 m (νNCN); 1082 vs (νSiO). Elemental analysis: (%, Anal. Calc. for $C_{18}H_{22}N_2O_{11.5}PSSi_6$) C, 30.97 (31.7); H, 4.01 (3.25); N, 4.03 (4.11); S, 4.35 (4.70).

2.2.10. Preparation of XGPtu[Pd]

A total of 500 mg (1.01 mmol) of SiPtu were dissolved in 25 ml of dry ethanol. This solution was added to 90 mg (0.5 mmol) of $PdCl_2$ and refluxed until the complete dissolution of the solid. The resulting orange solution was then filtered and dried, to give an orange solid. A total of 1.057 g (5.07 mmol) of TEOS and 10 ml of ethanol were added to the solid. To this solution, 2.27 mg (0.061 mmol) of NH_4F dissolved in 0.42 ml of water were added dropwise. After 30 min an orange gel formed. The gel was left to dry for 1 week and then roughly crushed, washed with boiling ethanol and diethylether and dried in vacuo to give small transparent orange monoliths. A total of 804 mg of solid were obtained, 102.8% yield calculated on **10** SiO$_2$·[SiO$_{3/2}$(CH$_2$)$_3$NHC-(S)NH(CH$_2$)$_2$PPh$_2$]$_2$(PdCl$_2$). IR (cm^{-1}, KBr pellet): 3393 vs, br (νOH, νNH); 3058 w (νCH arom); 2981 w, 2943 w (νCH aliph.); 1598 s (νNCN); 1071 vs (νSiO).

2.2.11. Preparation of XGPtu[PdCo]

A total of 500 mg (1.01 mmol) of SiPtu were dissolved in 25 ml of dry ethanol. To this mixture, 90 mg (0.5 mmol) of $PdCl_2$ were added and the solution was refluxed until complete dissolution of the solid. To the warm solution, 121 mg (0.5 mmol) of $CoCl_2{\cdot}6H_2O$ were added. The solid dissolved rapidly and the solution color turned green. The solution was then filtered and dried, to give a green solid. A total of 1.057 g (5.07 mmol) of TEOS and 10 ml of ethanol were added to the solid. To this solution, 2.27 mg (0.061 mmol) of NH_4F dissolved in 0.42 ml of water were added dropwise. After 30 min a greenish yellow gel formed. The gel was left to dry for 1 week and then dried in vacuo to give small transparent green monoliths. This xerogel, if washed with water, releases all the Co(II) ions turning to orange; the same happens to a less extent by using ethanol. A total of 890 mg of solid were obtained, 105% yield calculated on **10** SiO$_2$·[SiO$_{3/2}$(CH$_2$)$_3$NHC(S)NH(CH$_2$)$_2$PPh$_2$]$_2$(PdCoCl$_4$). IR (cm^{-1}, KBr pellet): 3391 vs, br (νOH, νNH); 3058 w (νCH arom); 2947 w (νCH aliph.); 1597 m (νNCN); 1095 vs (νSiO).

2.2.12. Anchoring of Rh(I) and Pd(II) on the XGPtu xerogel: preparation of Rh/XGPtu and Pd/XGPtu

Rhodium and palladium complexes were anchored on XGPtu by stirring, for some hours, a suspension of thiourea-functionalized material in a CH_2Cl_2 solution

of a weighted excess of [{Rh(cod)Cl}$_2$] or [Pd(NCPh)$_2$Cl$_2$]. The solid was then filtered in the air and washed repeatedly with dichloromethane. The anchoring yield was calculated in the following way. After the anchoring reaction, the solution was filtered quantitatively and the solvent evaporated in vacuum. The residual metal precursor was weighted and its quantity subtracted to the starting amount, obtaining the approximate anchored quantity. The maximum theoretical anchored amount of complex was calculated considering the mol g^{-1} of thioureic functions (from the XGPtu molecular formula) and assuming the 1:1 Rh–S coordination and the 1:2 Pd–S coordination. In the case of Rh/XGPtu, the anchoring yield was measured, with the same contact time (2 h), for xerogels with different aging times.

2.2.12.1. Rh/XGPtu. A total of 300 mg (0.44 mmol of S) of XGPtu were grinded and suspended in a solution of 173 mg (0.35 mmol) of [{Rh(cod)Cl}$_2$] in 10 ml of CH_2Cl_2. The suspension was stirred for 10 h, the solid filtered and washed repeatedly with CH_2Cl_2. Anchoring yields (aging time): 99% (6 days); 94% (11 days); 72% (42 days); $<10\%$ (63 days). IR (cm^{-1}, KBr pellet): 3245 m (νOH, νNH); 3054 w (νCH arom.); 2976 w, 2940 w (νCH aliph.); 2879 w (νCH cod); 1589 s (ν_{as}NCN); 1089 vs (νSiO). XPS interatomic ratios (aging time 6 days): Rh/N/P/S/Si/Cl: 1/1.7/1.1/1.1/7.1/1.1. XPS Binding Energies (eV): P2p 132.1; S2p 162.8; N1s 399.9; Rh3d$_{5/2}$ 308.7; Cl2p 198.5.

2.2.12.2. Pd/XGPtu. A total of 500 mg (0.73 mmol of S) of XGPtu were grinded and suspended in a solution of 280 mg (0.8 mmol) of (PhCN)$_2$PdCl$_2$ in 10 ml of CH_2Cl_2. The suspension was stirred for 10 h. The solid was then filtered and washed repeatedly with CH_2Cl_2. Anchoring yield 50%. IR (cm^{-1}, KBr pellet): 3299 m (νOH, νNH); 3071 w, 3057 w (νCH arom.); 2978 w (νCH aliph.); 1559 m (ν_{as} NCN); 1089 vs (νSiO).

2.2.13. Preparation of [($xSiO_2 \cdot SiO_{3/2}(CH_2)_3NHC(S)NHPh)_nPdCl_2$] ($n=2$, $x=10$, XGphtu[Pd2]; $n=4$, $x=20$, XGphtu[Pd4]; $x=30$, $n=6$, XGphtu[Pd6]

General conditions for gel formation were: H_2O–EtO = 1, [Si] $\approx$ 1 mol l^{-1}, (TEOS)–ligand = 5, Si–F = 100 ($n=4$, 6), 10 ($n=2$). A total of 200 mg of (PhCN)$_2$PdCl$_2$ were dissolved in 10 ml of CH_2Cl_2. To this solution were added 372 ($n=2$), 745 ($n=4$) or 1116 ($n=6$) mg of Siphtu dissolved in another 10 ml of CH_2Cl_2. The solution containing the complex was evaporated to dryness. The orange solid was dissolved in 7, 14 or 21 ml of CH_3OH and transferred to a 100 ml becker. A total of 1085, 2170 or 3255 mg of TEOS were added under stirring and a solution of 23.2, 4.63 or 6.95 mg of NH_4F in 0.43, 0.86 or 1.30 ml of water was rapidly added dropwise to the orange solution. A gel formed after 10–15 min. Orange, transparent, brittle xerogels were obtained by natural drying in 20 days.

2.2.13.1. XGphtu2Pd. IR (cm^{-1}, KBr pellet): 3250 s, br (νOH, νNH); 1587 s (ν_{as}NCN); 1087 vs (νSiO).

2.2.13.2. XGphtu4Pd. IR (cm^{-1}, KBr pellet): 3250 s, br (νOH, νNH); 1575 s (ν_{as}NCN); 1085 vs (νSiO).

2.2.13.3. XGphtu6Pd. IR (cm^{-1}, KBr pellet): 3400 s, br (νOH, νNH); 1566 m (ν_{as}NCN); 1092 vs (νSiO).

2.2.14. Hydrogenation of phenylacetylene

Hydrogenation reactions were carried out in a Schlenk tube connected to an atmospheric pressure gas burette. The catalyst was disareated and then 20 ml of dry ethanol and 0.5 ml (4.4 mmol; substrate–[Pd] = 100) of phenylacetylene were added. The solution was thermostated at 40–50°C and left to react for 15–24 h.

The final product mixture was filtered (in the case of the supported catalysts) and analyzed by GC.

2.2.15. Hydroformylation of styrene

In a typical run, distilled styrene (2.3 ml), toluene (3 ml) and the catalyst were introduced under nitrogen in the autoclave to achieve the desired styrene–Rh ratio (200–300). After some pressurization and evacuation cycles at -20°C, the autoclave was charged at room temperature with a 1:1 hydrogen carbon monoxide mixture at 60 atm of pressure. The reaction mixture was stirred at 80°C for 5–7 h and then analyzed by GLC. In the case of the supported catalysts, the powder was recovered by filtration in the air and washed with dichloromethane to be reused in a further run.

The xerogel Rh/XGPtu has been used in ten runs for a reaction time of 5 h each. A total of 150 mg of catalyst were used at the first run and 30 mg were left at the tenth (because of filtration loss and sampling for FTIR and XPS analysis). Disregarding the Rh leaching, the styrene–Rh ratio was 130 at the first run and 590 at the tenth run.

*2.3. Crystal structure determination of complexes **1**, **2** and **3***

The intensity data of **1** and **3** were collected at room temperature on a Philips PW 1100 single-crystal diffractometer using a graphite monochromated Mo–K$_\alpha$ radiation and the $\theta/2\theta$ scan technique. The intensity data of **2** were collected at room temperature on a Enraf Nonius CAD 4 single-crystal diffractometer using a graphite monochromated Cu–K$_\alpha$ radiation and the $\theta/2\theta$ scan technique. Final unit cell parameters were obtained from a least-squares refinement using 24 (**1**, **2** and **3**) reflections. Crystallographic and experimental details for both structures are summarized in Table 1.

Table 1
Experimental data for the X-ray diffraction studies of **1**, **2**, **3**

Formula	$[C_{42}H_{42}N_4P_2S_2Pd]$ $Cl_2{\cdot}6CHCl_3$	$[C_{42}H_{42}N_4P_2S_2Pd]Cl_2{\cdot}C_2H_6O$	$[C_{42}H_{42}N_4P_2S_2Pd]$ $CoCl_4{\cdot}CHCl_3{\cdot}2C_2H_6O$
Formula weight	1622.46	952.22	2494.98
Temperature	293(2)	293(2)	293(2)
Wavelength	0.71073	1.54183	0.71073
Crystal system	Monoclinic	Monoclinic	Triclinic
Space group	$P2_1/n$	$P2_1/c$	$P\bar{1}$
Unit cell dimensions			
a (Å)	14.909(4)	9.407(2)	14.204(5)
b (Å)	19.212(5)	26.954(6)	16.610(6)
c (Å)	12.364(3)	18.062(4)	13.984(4)
α (°)			105.07(2)
β (°)	90.23(2)	101.36(2)	119.10(3)
γ (°)			77.89(2)
V (Å^3)	3541(2)	4490(2)	2770(2)
Z	2	4	1
$D_{calc.}$ (Mg m^{-3})	1.521	1.409	1.496
Absorption coefficient μ (mm^{-1})	1.156	6.268	1.135
$F(000)$	1624	1960	1270
Crystal size (mm)	$0.10\times0.21\times0.15$	$0.13\times0.23\times0.34$	$0.15\times0.28\times0.31$
θ range (°)	3.01–25.03	3.28–70	3.02–25
Index ranges	$-17\le h\le17$, $0\le k\le22$, $0\le l\le14$	$-11\le h\le11$, $-28\le k\le32$, $-18\le l\le22$	$-16\le h\le14$, $-19\le k\le19$, $0\le l\le16$
Reflections collected	6514	8783	9719
Independent reflections	6221 ($R_{int}=0.0538$)	8514 ($R_{int}=0.0486$)	9719 ($R_{int}=0.0000$)
Observed reflections [$I>2\sigma(I)$]	2025	4941	2045
Refinement method	Based on F^2	Based on F^2	Based on F^2
Data/restraints/parameters	6221/0/360	8514/0/501	9719/0/422
Goodness-of-fit on F^2	0.866	1.048	0.959
Final R indices [$I>2\sigma(I)$]	$R_1=0.0665$, $wR_2=0.1589$	$R_1=0.0528$, $wR_2=0.1396$	$R_1=0.0978$, $wR_2=0.2023$
R indices (all data) [a]	$R_1=0.2324$, $wR_2=0.2374$	$R_1=0.1103$, $wR_2=0.1981$	$R_1=0.4974$, $wR_2=0.3837$
Largest difference peak and hole (e Å^{-3})	0.613 and −0.477	1.141 and −1.025	1.159 and −0.700

[a] $R_1=\Sigma\|F_o-F_c\|/|\Sigma(F_o)wR_2=[\Sigma[w(F_o^2-F_c^2)^2]/\Sigma[w(F_o^2)^2]]^{1/2}$.

Data were corrected for Lorentz and polarization effects in the usual manner. A correction for absorption was made for both complexes [maximum and minimum value for the transmission coefficient was 1.000 and 0.5401 (1), 1.000 and 0.6389 (**2**) and 1.000 and 0.3966 (**3**) [15].

The structures were solved by Patterson and Fourier methods and refined by full-matrix least-squares procedures (based on F_o^2) with anisotropic thermal parameters in the last cycles of refinement for all the non-hydrogen atoms excepting for the atoms of one molecule of $CHCl_3$ in **1** where each Cl atom was found disordered and distributed in three positions of occupancy factors 0.33, excepting for the atoms of the solvent in **2**, whereas in **3** only the Pd, N, P, S and the C1, C2, C3 atoms, those of $CoCl_4$ moiety and the atoms of the three molecules of the solvents were refined anisotropically.

In all three structure, the hydrogen atoms (except those of the solvent molecules) were introduced into the geometrically calculated positions and refined *riding* on the corresponding parent atoms. In the final cycles of refinement, a weighting scheme $w=1/[\sigma^2F_o^2+(0.1061P)^2]$ (**1**), $w=1/[\sigma^2F_o^2+(0.0953P)^2+3.2539P]$ (**2**) and $w=1/[\sigma^2F_o^2+(0.1360)^2+6.1527P]$ (**3**) where $P=(F_o^2+2F_c^2)/3$ was used.

All calculations were carried out on the DIGITAL AlphaStation 255 computers of the 'Centro di Studio per la Strutturistica Diffrattometrica' del CNR, Parma, using the SHELX-97 systems of crystallographic computer programs [16].

3. Results and discussion

3.1. Syntheses and characterizations of ligand and complexes

The ligand $Ph_2PCH_2CH_2NHC(S)NHPh$ (Ptu) is prepared by the reaction of the amine $Ph_2PCH_2CH_2NH_2$ and the isothiocyanate PhNCS in ethanol. It is a stable, white solid, soluble in polar and chlorinated solvents. By the reaction with Pd(II) and Rh(I) chloride precursors, the complexes $[(Ptu)_2Pd]Cl_2$ (PdPtu) and [(Ptu)Rh(cod)]Cl (RhPtu) are formed. Ptu is

coordinated through the P and S atoms forming seven-membered rings (vide infra). Spectroscopic evidence for the P,S-coordination comes from the lowfields shift of the ^{31}P-NMR resonance in the complexes [δ 28.3 in PdPtu and 33.1 ($^{1}J_{Rh,P} = 150$ Hz) in RhPtu] with respect to the free molecule (-21.1), and from the blue shift of the ν(NCN) IR band (1575 cm^{-1} in PdPtu, 1572 in RhPtu, 1536 in Ptu). Moreover, in the ^{1}H-NMR spectra, the significant shifts to high frequencies of the peaks due to the NH protons suggest thiourea S-coordination, particularly for the NH group of the chelation ring which moves from δ 6.27 (Ptu) to 10.50 (PdPtu) and 9.96 (RhPtu).

The ^{1}H-NMR spectra of the complexes $[(Ptu)_2Pd]Cl_2$ and [(Ptu)Rh(cod)]Cl show two CH_2CH_2 peaks, which remain broad in the range of temperatures 330–233 K, indicating a low-barrier dynamic behavior for these groups. Regarding the PhNHC(S) moiety, which could be present in two conformers (*syn–anti*), only one N*H* peak is present even at 233 K. In the Rh(I) complexes, the vinylic protons of the coordinated cod ligand give rise to two broad peaks corresponding to the two halves of the ligand in *trans*, respectively to the P and S atoms.

The Pd and Rh complexes were reacted with $CoCl_2$ trying to obtain bimetallic complexes by opening the chelation ring. However, $CoCl_2$ prefers to add Cl^- anions resulting in the formation of the ion-pair complexes $[(Ptu)_2Pd][CoCl_4]$ (PdPtuCo) and $[(Ptu)Rh(cod)]_2[CoCl_4]$ (RhPtuCo). The ^{1}H-NMR of these products shows broad and overlapping peaks, probably because of the presence of the Co(II) paramagnetism. Nevertheless, in the case of the Rh(I) compound, ^{31}P-NMR shows a sharp doublet (δ 33.1, $^{1}J_{P,Rh} = 150$ Hz) indicative of the Rh–P coordinative interaction), whereas the Pd(II) complex shows a large peak (δ 36.0, $\Delta\nu_{1/2} = 170$ Hz) at room temperature. By lowering the temperature to 253 K, a minor sharp peak appears at δ 31.0, close to the value of the chloride derivative (δ 32.5 at 253 K). This suggests that, in solution at least two intercoverting species could be present, one being the Pd bis-chelate cationic complex, and the other probably containing Co(II)–P interactions, giving account for the ^{31}P line broadening [by the way, the ^{31}P resonance of $(Ph_3P)_2CoCl_2$ is not detectable].

Both Rh–Co and Pd–Co ion-pair complexes can be retransformed into the parent complexes, RhPtu and PdPtu, by addition of water to their green chloroform solutions. The aqueous layer becomes colored in pink, indicating the presence of the Co(II) aquo-cation, while the chloroform layer turns yellow. In the case of RhPtu, the chloride ligand is easily displaced by PF_6^-, by dissolving the complex in a concentrated solution of KPF_6, giving the cationic complex $[(Ptu)Rh(cod)]PF_6$ (RhPtuPF6).

3.2. X-ray structural results

Views of the structures of the Pd complexes **1**, **2** and **3** are shown in Figs. 1–3, respectively. Selected interatomic distances and angles regarding the chelation rings are reported in Tables 2 and 3. In all the three complexes the two bidentate ligands form two heptaatomic chelation rings with the donating atoms in *trans* disposition and adopt a cyclohexane-like, *quasi*-boat conformation, when considering the rigid thiourea group to contribute with one side to the ring, as outlined in the scheme attached to Table 3.

As the Ptu ligand can adopt a *syn* or an *anti* configuration regarding the thiourea moiety PhNHC(S)–, complex **1** contains *syn*-Ptu, whereas complex **2** exhibits both the two arrangements. On the other hand, the structure of **3** contains two independent molecules differentiated just by the *syn–anti* configuration. In all cases, the *syn* disposition, which should be more sterically hindered, appears to be driven by the formation of bifurcated N–H···Cl hydrogen bonds with isolated chloride ions, as in **1** and **2**, or with the tetrachlorocobaltate anion, as in **3**.

Regarding the bis-chelation configuration, while in complexes **1** and **3** the two ligands are *centrosymmetricallly* related, in complex **2** they are folded by the same side with respect to the coordination plane, in an *umbrella* configuration sketched in Scheme 2. These different configurations appear to affect slightly the coordinative interactions, as in **2**, differently from the other complexes, the Pd–S bond distances are significantly longer than the Pd–P ones.

This could also be related to the presence, in complex **2**, of the Pd···Cl(1) interaction [3.026(2) Å], which appears to induce a certain degree of distortion of the square planar geometry around the metal. In fact, the resulting coordination environment is that of an incipient trigonal bipyramid, with the two phosphorus atoms occupying the apical positions [P–Pd–P 179.5(1), S–Pd–S 160.6(1)°]. Furthermore, the proximity of the chlorine atom Cl(1) to the metal center causes significant modifications in the geometry of the two chelation rings. In fact, the two methylene groups C(2a) and C(2b) close to palladium move slightly away, as evidenced by the values of the distance h' and of the torsion angles α, β and η in Table 3. However, two weak interactions take place between the methylene groups and the chlorine atom [e.g. Cl(1)···C(2b) 3.662(5) Å, Cl(1)···H(2b1)–C(2b) 132.5(5)°].

Moreover, the planarity of the thiourea moieties in **2** appears slightly affected by the *umbrella* configuration, as evidenced by the values of the torsion angle γ. In addition, the values of the dihedral angle between the main coordination plane and thiourea moieties, which range between 43.6(3) and 47.5(5) in **1** and **3**, are significantly raised in **2** [53.3(1) (*syn*) and 57.5(1)° (*anti*)].

Packing in compound **2** is mainly driven by a network of hydrogen bonds involving Cl(2), which interact with N(1a) [3.217(4) Å, 154.4(4)°] and N(2a) [3.167(5) Å, 156.7(5)°] in a bifurcated fashion (determining the *syn* arrangement) and with N(1b) [3.233(4) Å, 132.9(4)°] of an adjacent molecule. The oxygen of the ethanol molecule behaves as acceptor in the H-bond interaction N(2b)···O(1s) [2.799(7) Å, 154.5(5)°].

In compound **3**, the complex molecule containing the *syn* thiourea moieties interacts through the N–H groups with two chlorine of the $[CoCl_4]^{2-}$ anion [N(1a)···Cl(4) 3.24(2) Å, 146(2)°; N(2a)···Cl(1) 3.17(2), 154(2)°]. On

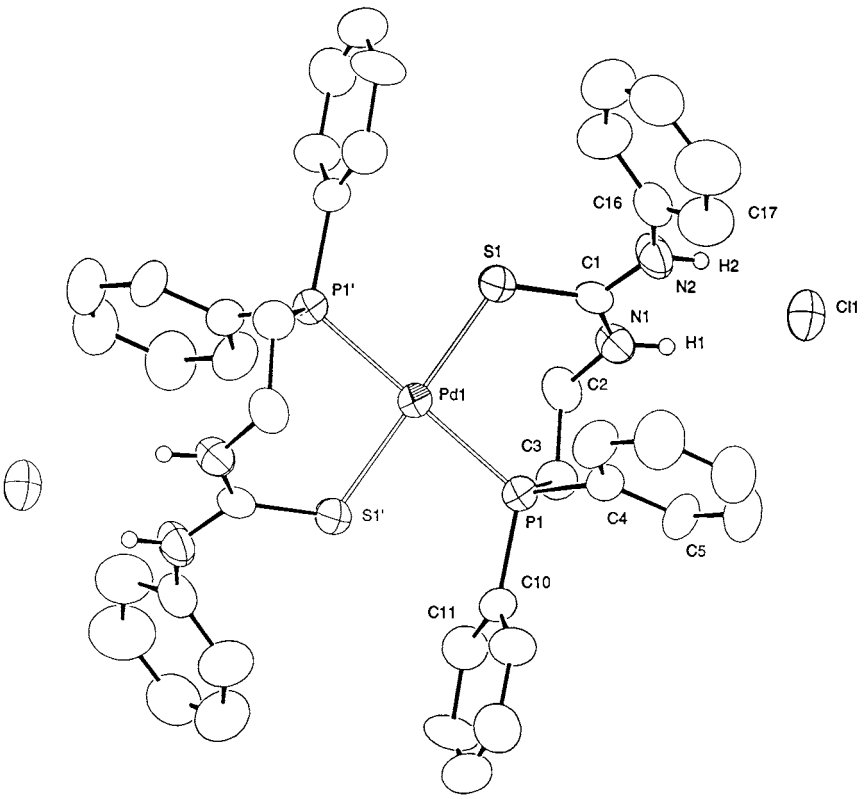

Fig. 1. ORTEP diagram of the complex $[Pd(Ptu)_2]Cl_2 \cdot 6CHCl_3$ (**1**) with the atomic numbering scheme, showing 30% probability thermal ellipsoid.

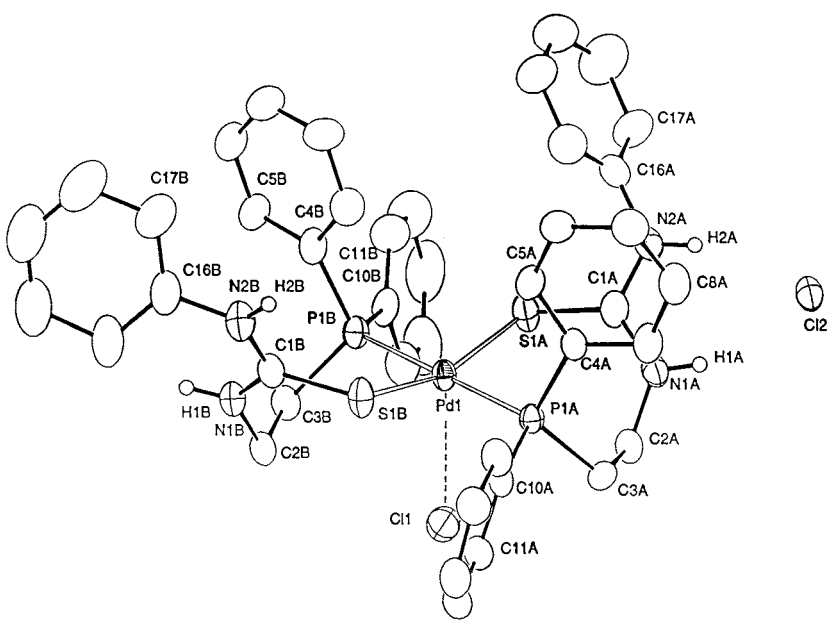

Fig. 2. ORTEP diagram of the complex $[Pd(Ptu)_2Cl]Cl \cdot EtOH$ (**2**) with the atomic numbering scheme, showing 30% probability thermal ellipsoid.

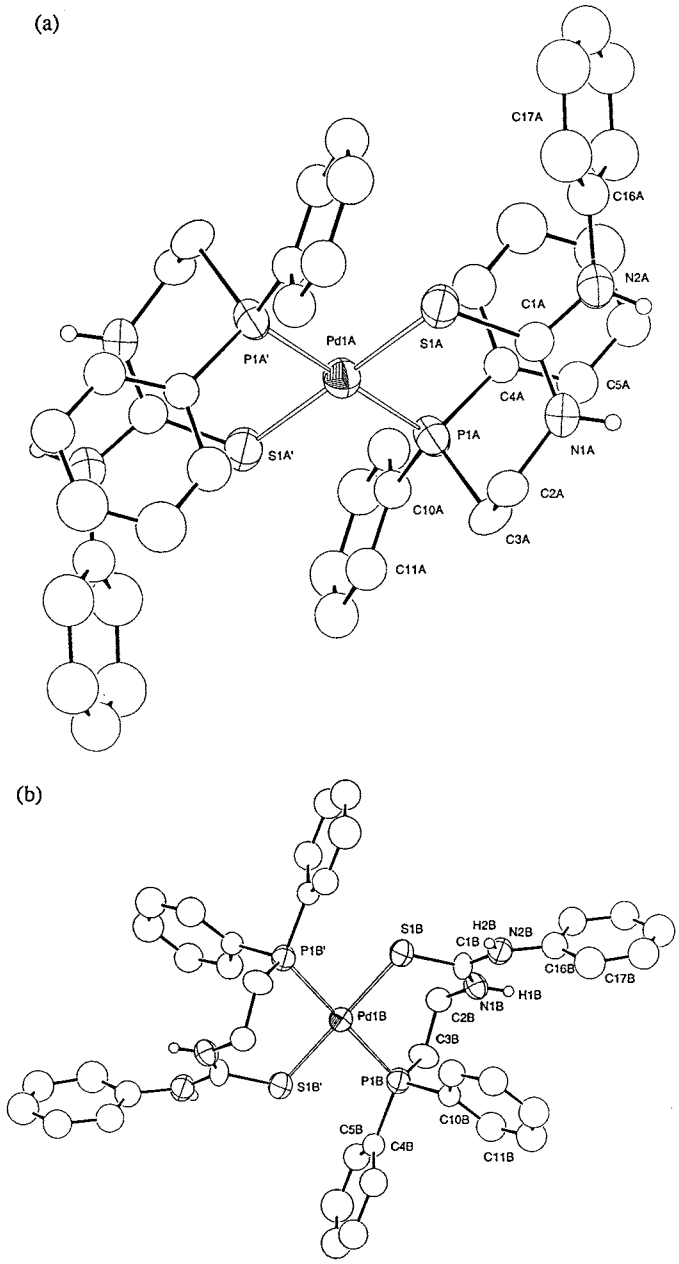

Fig. 3. ORTEP diagram of the complex $[Pd(Ptu)_2][CoCl_4]\cdot CHCl_3\cdot 2EtOH$ (**3**) with the atomic numbering scheme, showing 30% probability thermal ellipsoid: (a) molecule A (*syn* conformation of the thiourea groups); (b) molecule B (*anti* conformation).

the other hand, the second molecule containing the *anti* thiourea groups interacts through the N–H groups with the two ethanolic oxygens [N(1b)···O(2s) 2.84(2) Å, 141(2)°; N(2b)···O(1s) 2.86(3) Å, 162(2)°].

Packing in complex **1** appears quite different being mainly due to the presence of six chloroform molecules which give rise to a sort of clathrate compound. There is a number of Cl···Cl interactions between adjacent $CHCl_3$ molecules lying in the same range of distances (3.59–4.07 Å) found in the crystal structure of pure chloroform [17]. Also in this case, there is a bifurcated hydrogen bond couple N–H···Cl between the *syn* thiourea group and the chloride ion [N(1)···Cl 3.18(1) Å, 156(1)°; N(2)···Cl 3.16(1) Å, 158(1)°]. The chloride ion is also bound weakly to two chloroform molecules through Cl···H–CCl_3 interactions [Cl···C(1b) 3.61(2), Cl···C(1a) 3.47(2) Å].

3.3. Sol-gel preparation of silica supported Ptu complexes

In order to produce the same Ptu complexes of Rh(I) and Pd(II) tethered to silica xerogels, the ligand $(EtO)_3Si(CH_2)_3NHC(S)(CH_2)_2PPh_2$ (SiPtu), or its metal complexes, were sol-gel processed with tetraethyl orthosilicate (TEOS), in the desired ratio. In particular, the $5SiO_2\cdot SiO_{3/2}(CH_2)_3NHC(S)NH(CH_2)_2PPh_2$ (XGPtu) xerogel was prepared, with a Si–S ratio equal to 6, which allows satisfactory spectroscopic characterization of the tethered species.

We used two ways of anchoring a metal complex on silica gels: the first one (method A) implies the suspension of XGPtu in a solution containing the suitable metal precursor; the second way (method B) consists in the reaction of a metal precursor with the Siptu ligand in a well defined stoichiometric ratio and in sol-gel processing the obtained complex with TEOS. In both cases, the integrity of the tethered ligand in the gels was confirmed by the presence in their IR spectra of its typical bands. Moreover, in the case of the complexes the expected blue shift for the ν_{as}(NCN) band was observed.

With method A, the metal precursors react firstly with the surface ligand functions, and then diffuse into the matrix to reach the inner functional groups. This was proved previously, in the case of Rh on XGphtu, by comparing the Si–Rh ratios obtained by EDX (bulk) and XPS (surface) semiquantitative analysis [8]. In the present work, we found that the amount of the adsorbed metal depends not only on the contact time between the xerogel and the metal precursor solution, but also on the aging of the gel. In fact, for longer aging times, the metal loading strongly decreases, as reported in Table 4 for XGPtu and Rh(I). Complete coverage of all the thiourea functions by the metal ions is possible only for *young* xerogels, and not for *old* ones, probably owing to the reduction of the pore size. As a result, the metal-to-ligand ratio is out of strict control, being possibly higher in the surface and lower in the inner, with respect to that of the corresponding molecular complex (e.g. 2 in the case of $[Pd(Ptu)_2]Cl_2$). For *young* xerogels the anchoring yield can approach 100% in the case of Rh(I). In the case of Pd/XGPtu, instead, the anchoring yield is never 100% but spans from 50% (as for the materials used in catalysis) to 70–80%, suggesting that the 2/1 P–S/Pd coordination is

Table 2
Selected bond distances (Å) and angles (°) in the chelation rings of **1** [a], **2** [b] and **3** [a] (estimated standard deviations in parentheses; for the label keys see the scheme below Table 3)

	1 (*syn*)	**2** (ligand a, *syn*)	**2** (ligand b, *anti*)	**3** (complex a, *syn*)	**3** (complex b, *anti*)
Bond distances					
Pd–P	2.338(5)	2.316(2)	2.316(2)	2.359(6)	2.334(6)
Pd–S	2.327(5)	2.355(2)	2.355(2)	2.314(6)	2.337(6)
S–C(1)	1.711(10)	1.734(8)	1.745(7)	1.67(2)	1.73(2)
C(1)–N(1)	1.326(11)	1.327(9)	1.312(8)	1.29(2)	1.32(2)
C(1)–N(2)	1.325(11)	1.331(8)	1.338(9)	1.36(2)	1.32(2)
Bond angles					
Pd–P–C(3)	109.4(4)	113.3(2)	112.3(3)	107.7(3)	109.1(7)
P–Pd–S	94.7(1)	95.69(6)	94.53(7)	93.3(2)	95.7(2)
Pd–S–C(1)	116.8(3)	114.5(3)	114.8(2)	117(1)	117(1)
S–C(1)–N(1)	125.5(8)	122.8(6)	122.8(6)	131.2(2)	126(2)
N(1)–C(1)–N(2)	115.2(9)	117.1(7)	120.6(6)	111.2(2)	119(2)
S–C(1)–N(2)	119.2(8)	119.8(6)	116.5(5)	118(2)	114(2)

[a] Centrosymmetrical bis-chelation.
[b] Umbrella bis-chelation configuration (see scheme through the text).

Table 3
Pd···H contacts h', h'' (Å) and torsion angles α–η (°) in the chelation rings of **1**, **2** and **3** (estimated standard deviations in parentheses; for the label keys see the schemes below) [a]

	1	**2** (ligand a)	**2** (ligand b)	**3** (complex a)	**3** (complex b)
h'	2.94(1)	3.20(1)	3.12(1)	2.84(2)	3.06(2)
h''	3.03(1)	3.09(1)	2.85(1)	3.17(2)	2.92(3)
α	11.5(4)	−8.1(2)	−3.7(2)	20(1)	4(1)
β	41(1)	59.6(5)	60.9(5)	34(3)	46(3)
γ	1(2)	−3.4(8)	−9.3(7)	0(3)	1(3)
δ	−96(1)	−96.1(6)	−92.8(6)	−97(2)	−96(3)
ε	58(1)	55.4(5)	60.2(5)	65(2)	56(2)
ζ	41.8(8)	42.2(4)	39.6(4)	36(2)	42(2)
η	−69.4(4)	−57.5(2)	−59.9(2)	−72(1)	−63(1)

[a]

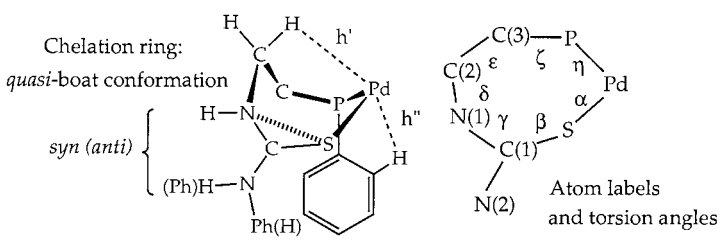

hardly reached, as it requires the close presence of two Ptu functions in the xerogel matrix.

With method B, the metal complex is formed in solution and keeps its structural features when homogeneously dispersed in the xerogel, allowing to control both the stoichiometry of the complex and the silica to metal ratio.

In our previous studies with monodentate thioureas [4,6b,8], we always used method A to anchor both Pd(II) and Rh(I) complexes. Method B was found to be ineffective in the case of Rh(I), probably because the fluoride ions (used as catalyst for the sol-gel process) are withdrawn from their task by interactions with the metal centers. Only with higher F^-–Si ratio it was possible to obtain gelation, but the formation of a genuine, homogeneous gel was never achieved because of precipitation of oligomeric substances.

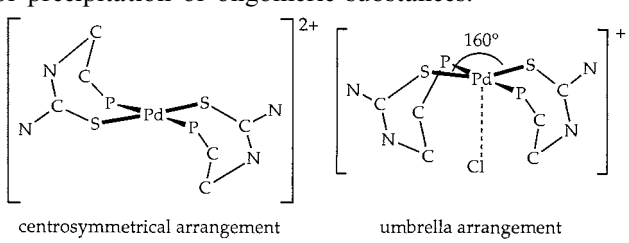

Scheme 2.

Table 4
Anchoring yield [a] of Rh(I) on XGPtu in dependence on the aging time of the xerogel

Aging time (days)	Anchoring yield (%)
6	99
11	94
42	72
63	<10

[a] Calculated according to the method reported in Section 2.2.12.

Table 5
Results [a] of the homogeneous hydrogenation tests with the Pd complexes

	PdPtu	PdPtuCo
Phenylacetylene	91	0
Styrene	8	79
Ethylbenzene	<1	21

[a] Percentage of the substance in the product mixture.

Table 6
Results [a] of the homogeneous hydroformylation tests with the Rh complexes

	RhPtu	RhCoPtu	$RhPtuPF_6$
Styrene	99	0	1
iso aldehyde	0	92	80
n aldehyde	0	4	18
Ethylbenzene	< 1	4	1

[a] Percentage of the substance in the product mixture.

In this work we prepared the Rh(I) xerogels using method A and the Pd(II) xerogels using both methods. The xerogels obtained by method A are yellow in the case of rhodium and orange in the case of palladium. The gelation of the preformed 2:1 complex of SiPtu with Pd(II) does not need a higher quantity of F^- catalyst (probably because the Pd(II) center was protected by the ligands) and gives orange, transparent xerogel monoliths. When gelling the complex of SiPtu with Pd(II) and $CoCl_4^-$ as counterion, more water was needed (instead of more catalyst) for gelation. A bright green material is obtained which, if washed with water, completely loses Co(II) turning orange.

In order to compare the behavior of the Ptu ligand with that of simple thiourea ligands [4], we prepared Pd containing xerogels following method B, using $(EtO)_3Si(CH_2)_3NHC(S)NHPh$ (Siphtu) in different S–Pd ratios (2, 4, 6).

3.4. Catalytic activity tests on Ptu molecular complexes

The catalytic activity of the complexes PdPtu and PdPtuCo was tested on the hydrogenation of phenylacetylene to styrene and ethylbenzene at atmospheric pressure. As shown in Table 5, PdPtu exhibited a very low activity, but the substitution of Cl^- with the non coordinating $CoCl_4^-$ anion resulted in a dramatic increasing of the hydrogenating ability. This suggests the existence in solution of interactions between the Cl^- ion and the Pd(II) center which could hinder the coordination of the substrate. This kind of interaction could be similar to that observed in the solid state structure of compound **2**. The mechanism of this reaction has not been investigated. Apparently, the Pd complexes can be recovered intact from the reaction mixture, but we cannot exclude the formation of trace amounts of colloidal metal particles, responsible for the observed catalytic activity.

A similar behavior was found for the complex Rh-Ptu, which was not active in the hydroformylation of styrene. Again, by substituting the Cl^- anion with PF_6^- or $CoCl_4^-$, complete conversion of styrene to aldehydes was observed (Table 6). It is also interesting to note the high selectivity of the Rh–Co compound towards the *iso* aldehyde (at 80°C, $iso/n = 23$; for comparison, the complex [(PhNHC(S)NHPh)Rh(cod)Cl] showed $iso/n \approx 2$ [8]). After the catalysis, rhodium carbonyl complexes were recovered by precipitation with a mixture of Et_2O–hexane. Their IR spectra in the carbonyl region showed the typical two-band pattern of *gem*-$(CO)_2$ species (2024, 1975 cm^{-1} for the chloride and 2038, 1980 cm^{-1} for the chlorocobaltate derivative).

3.5. Catalytic tests with anchored complexes

We prepared and tested in catalysis the following materials: (i) Rh/XGPtu and Pd/XGPtu obtained by anchoring of the metal species on the XGPtu xerogel (method A); (ii) two Pd(II) containing xerogels using the preformed **2:1** SiPtu complex (method B), the one with Cl^- as anion (XGPtu[Pd]) and the other with $CoCl_4^-$ (XGPtu[PdCo]; (iii) three Pd(II) containing xerogels using preformed Siphtu complexes (method B), with a S–Pd ratio of 2 (XGphtu[Pd2]), 4 (XGphtu[Pd4]) and 6 (XGphtu[Pd6]) (method B). All the xerogel materials were prepared with a Si–S ratio equal to 6 (TEOS–thiourea = 5).

3.5.1. Hydroformylation of styrene using Rh/XGPtu

The Rh(I) containing xerogel Rh/XGPtu was prepared by suspending XGPtu (dried for 6 days) in a CH_2Cl_2 solution of $[\{Rh(cod)Cl\}_2]$. This xerogel is able to effectively convert styrene to a mixture of *iso*/*n* aldehydes and is easily recovered by filtration. The surface atomic ratios resulted from XPS analysis are reported in Table 7, together with those found after the first, fifth and tenth catalytic runs.

The activity of Rh/XGPtu is in contrast with that of the model compound [(Ptu)Rh(cod)]Cl, which is com-

pletely inactive. We can interpret this result in two ways: (i) the silica surface is able to interact with the Cl^- ion in order to keep it far away from the catalytic center or (ii) Rh(I) is leached in solution in the form of a complex with CO and/or styrene (or its aldehydes) which is active in the hydroformylation reaction. In this regard, it seems from the XPS data (Table 7) that surface Rh leaching is limited compared to similar thiourea xerogels [6b, 8]. This was confirmed by EDX investigations which showed the bulk Si–Rh atomic ratio to be constant after the catalytic runs. The *iso*/*n* ratio was also found to be constant with the recycling of the catalyst (mean value 2.3 ± 0.2). This is consistent with very low metal leaching, as for thiourea modified xerogels, we observed a correlation between the surface Rh leaching and the raising of the *iso*/*n* ratio [6b, 8]. In this case, a constant *iso*/*n* ratio suggests a limited surface leaching, lower than the intrinsic error (10%) of the XPS obtained interatomic ratios. However, the decomposition of the anchored complex becomes apparent at the tenth run. Evidently, leaching occurs, even if to a limited extent, therefore we cannot exclude that the released metal species do not contribute to the observed catalytic behavior.

Regarding the anchored metal species, as was already found in the above mentioned works, the cod ligand is substituted promptly by two CO molecules, as it is clear from the appearance of the two-band pattern due typically to *gem*-$(CO)_2$ rhodium species (2076, 1996 cm^{-1}). It is to remark that by treating a solution of the cod-complex RhPtu with CO, nearly the same bands are observed (2072, 1996 cm^{-1}). The same bands are still present after subsequent catalytic runs, showing the stability of the anchored species which seems not to transform in a thioureato complex as it was found for XGbztu and XGphtu xerogels [6b, 8].

XPS binding energies are reported in Table 8. The values of P and S binding energies in the supported complex are in agreement with those observed in the model compound RhPtu, whereas N and Cl binding energies slightly differ, this discrepancy being attributable to matrix effects. After five catalytic runs, the supported catalyst shows a change in the binding energy of the P atom, probably due to the substitution of the cod ligand by two CO ligands. After ten cycles the surface metal complexes appear unaffected by any significant modification, as observed also by FT-IR spectroscopy.

Table 7
XPS atomic ratios in the Rh/XGPtu catalyst before and after the catalytic runs

	Rh	N/Rh	P/Rh	S/Rh	Si/Rh
Rh/XGPtu	1	1.7	1.1	1.1	7.1
First run	1	2.0	0.9	0.9	7.1
Fifth run	1	1.8	1.1	0.7	6.7
Tenth run	1	3.5	1.7	1.4	10

Table 8
XPS binding energies (eV) for the Rh/XGPtu catalyst before and after the catalytic runs

	Rh	P	N	S	Cl
RhPtu [a]	308.9	132.1	400.5	162.8	198.9
Rh/XGPtu	308.7	132.1	399.9	162.8	198.5
5th run	308.8	132.5	399.8	– [b]	198.6
10th run	308.7	132.6	399.7	162.6	198.5

[a] Reported for comparison.
[b] The S2p signal was affected by low signal to noise ratio, due to the scarce quantity of the sample.

3.5.2. Hydrogenation of phenylacetylene using Pd/XGPtu and related species

The Pd(II) containing xerogel XGPtu[Pd] and XGPtu[PdCo], obtained from the pre-formed complexes of SiPtu (method B), are completely inactive for the hydrogenation of phenylacetylene. XGPtu[Pd] is a bright orange and transparent material and keeps its physical appearance after the catalytic run. The same happens for XGPtu[PdCo], which is green.

On the other hand, the material obtained by anchoring Pd(II) on XGPtu from a solution of $(PhCN)_2PdCl_2$ (Pd/XGPtu, method A), is active after an induction period of ca. 30 min at 40°C, in the same way as the analogous materials obtained from the xerogels containing the –NHC(S)NHPh [1a] and –NHC(S)NHC(O)Ph fragments [1b]. It was demonstrated clearly that catalytic activity in the hydrogenation of phenylacetylene was possible because of the formation of Pd colloidal particles stabilized on the silica surface by the thiourea ligands. Also in the case of Pd/XGPtu, the formation of colloidal particles was observed; the xerogel color changed from orange to dark brown during the hydrogenation reaction. It is not clear if these particles are formed directly on the surface of the xerogels or if Pd(II) is first leached in solution, reduced by hydrogen and then readsorbed by the silica matrix. The fresh material, in fact, if suspended in an ethanol solution of phenylacetylene, slowly loses palladium. Filtering this solution and exposing it to hydrogen resulted in some reduction of the alkyne to styrene. After the first catalytic run, Pd/XGPtu is still active and does not leach palladium anymore. On the contrary, leaching was not observed for the XGPtu[Pd] material, which contains well defined molecular complexes and, as stated above, is inactive.

In order to gain more insight into the effect of the surrounding ligands on the formation of colloidal particles, we prepared XGphtu[Pd2], XGphtu[Pd4] and XGphtu[Pd6] by sol-gel processing the preformed Siphtu–Pd complexes with the S–Pd ratios of 2, 4 and

6, respectively. The infrared spectra of these materials exhibit significant differences in the thiourea bands, suggesting the formation of different complex species. The material XGphtu[Pd2] showed catalytic activity and also some darkening of its color, suggesting formation of colloidal Pd particles. Its activity, though, was lower than that of the catalyst obtained by anchoring Pd(II) with method A [4]. The conversion of half of the starting phenylacetylene to styrene was reached after 3 days of reaction. XGphtu[Pd4] was found less active and no darkening of its color or Pd(II) leaching in solution was observed. XGphtu[Pd6] showed extremely low activity, converting only the 3% of alkyne in more than 5 days of reaction. Even if a hexa-coordinated thiourea–Pd complex should be excluded, it seems that the two *redundant* ligands contribute to stabilize the Pd(II), avoiding its reduction and thus its catalytic activity.

4. Conclusions

The new thiourea–phosphine bidentate ligand Ptu gives a series of chelate complexes with Pd(II) and Rh(I) forming seven-membered chelation rings with a boat-like conformation. However, its coordination capability is far from being exploited fully and needs further investigation.

The catalytic activity in homogeneous hydrogenation and hydroformylation reactions of the Pd(II) and Rh(I) complexes resulted strongly dependent on the counteranion, being high only in the presence of non-coordinating anionic groups, such as PF_6^- and $CoCl_4^-$. Additional studies are needed to understand the grounds of this behavior and the relevant mechanism of the catalytic processes.

Regarding the SiPtu complexes tethered on silica via sol-gel procedures, two synthetic methodologies were used: anchoring of metal species on the functionalized silica xerogels (method A); sol-gel processing preformed metal complexes (method B). It has been ascertained that yield in anchored metal, amount of metal leaching and activity in catalysis depend strongly on the preparation methodology and this effect should be always taken into account when using such materials in catalysis.

5. Supplementary material

The supplementary material for all three structures includes the lists of atomic coordinates for the non-H atoms, of calculated coordinates for the hydrogen atoms, of anisotropic thermal parameters. The details of the crystal structure investigations are deposited to the Cambridge Crystallographic Data Center as supplementary publications no. CCDC-132016 (**1**), no. CCDC-132017 (**2**) and no. CCDC-132018 (**3**). Copies of the data can be obtained free of charge on application to CCDC, 12 Union Road, Cambridge CB2 1EZ, UK [fax: +44-1223-336033; e-mail: deposit@ccdc.cam.ac.uk].

Acknowledgements

Financial support from MURST (Rome) is gratefully acknowledged. The facilities of Centro Interdipartimentale di Misure (Università di Parma) were used for recording NMR and mass spectra.

References

[1] J.J.E. Moreau, M.W. Chi Man, Coord. Chem. Rev. 178–180 (1998) 1073.
[2] (a) R.H. Grubbs, Chemtech. (1977) 513. (b) Yu. I. Yermakov, B.N. Kuznetsov, V.A. Zkharov, Catalysis by Supported Complexes, Elsevier, Amsterdam, 1981. (c) B. Cornils, W.A. Herrmann, Applied Homogeneous Catalysis with Organometallic Compounds, vol. 2, VCH, Weinheim, 1996.
[3] (a) M.A. Cauqui, J.M. Rodriguez-Izquierdo, J. Non-Cryst. Solids 147 (1992) 148. (b) U. Schubert, New J. Chem. 18 (1994) 1049. (c) E. Lindner, R. Schreiber, T. Schneller, P. Wegner, H.A. Mayer, W. Göpel, C. Siegler, Inorg. Chem. 35 (1996) 514. (d) H. Schumann, M. Hasan, F. Gelman, D. Avnir, J. Blum, Inorg. Chim. Acta 280 (1998) 21, and references therein.
[4] C. Ferrari, G. Predieri, A. Tiripicchio, M. Costa, Chem. Mater. 4 (1992) 243.
[5] (a) M. Biagini Cingi, G. Peoni, G. Predieri, A. Tiripicchio, M. Tiripicchio Camellini, Gazz. Chim. Ital. 122 (1992) 521. (b) D. Cauzzi, G. Predieri, A. Tiripicchio, R. Zanoni, C. Giori, Inorg. Chim. Acta 221 (1994) 183.
[6] (a) D. Cauzzi, M.A. Pellinghelli, G. Predieri, A. Tiripicchio, Gazz. Chim. Ital. 123 (1993) 713. (b) D. Cauzzi, M. Lanfranchi, G. Marzolini, G. Predieri, A. Tiripicchio, M. Costa, R. Zanoni, J. Organomet. Chem. 488 (1995) 115.
[7] (a) E. Boroni, G. Predieri, A. Tiripicchio, M. Tiripicchio Camellini, Organometallics 11 (1992) 3456. (b) E. Boroni, G. Predieri, A. Tiripicchio, M. Tiripicchio Camellini, J. Organomet. Chem. 451 (1993) 163.
[8] D. Cauzzi, M. Costa, L. Gonsalvi, M.A. Pellinghelli, G. Predieri, A. Tiripicchio, R. Zanoni, J. Organomet. Chem. 541 (1997) 377.
[9] D. Cauzzi, G. Marzolini, G. Predieri, A. Tiripicchio, M. Costa, G. Salviati, A. Armigliato, L. Basini, R. Zanoni, J. Mater. Chem. 5 (1995) 1375.
[10] (a) K. Issleib, A. Kipke, V. Hahnfeld, Z. Anorg. Allg. Chem. 444 (1978) 5. (b) H. Oehme, R. Thamm, J. Prakt. Chem. 315 (1973) 526.
[11] (a) G. Kemp, A. Roodt, W. Purcell, K.R. Koch, J. Chem. Soc. Dalton Trans. (1997) 4481. (b) K.R. Koch, Y. Wang, A. Coetzee, J. Chem. Soc. Dalton Trans. (1999) 1013.
[12] (a) M. Gruber, P.G. Jones, R. Schmutzler, Phosphorus Sulfur Silicon 80 (1993) 195. (b) P. Bhattacharyya, A.M.Z. Slawin, M.B. Smith, D.J. Williams, D. Woolins, J. Chem. Soc. Dalton Trans. (1996) 3647. (c) S. Okeya, H. Shimomura, Y. Kushi, Chem. Lett. (1992) 2019. Other references of non structurally characterized products can be found in Beilstein: registry numbers: 6334221, 4175249, 6322671, 6327694, 5874279, 6327694, 6327816, 6330876, 6339300, 6351555, 7798905.

[13] (a) M.J. Baker, M.F. Giles, A.G. Orpen, M.J. Taylor, R. Watt, J. Chem. Soc. Chem. Commun. (1995) 197. (b) J.R. Dilworth, J.R. Miller, N. Wheatley, M.J. Baker, J.G. Sunley, J. Chem. Soc. Chem. Commun. (1995) 1579.
[14] T. Yamamoto, S. Sugiyama, K. Akimoto, K. Hayashi, Org. Prep. Proc. Int. 24 (1992) 346.
[15] (a) N. Walker, D. Stuart, Acta Crystallogr., Sect. A 39 (1983) 158. (b) F. Ugozzoli, Comput. Chem. 11 (1987) 109.
[16] G.M. Sheldrick, SHELXL-97 Program for the Refinement of Crystal Structures, University of Göttingen, Göttingen, Germany, 1997.
[17] R. Fourme, M. Renaud, C. R. Acad. Sci. Paris, Ser. A, 263b (1966) 69.